

## Resonant degenerate four-wave mixing in dense media

E. Pawelec, W. Gawlik, B. Samson, and K. Musioł  
*Instytut Fizyki, Uniwersytet Jagielloński, PL-30-059 Kraków, Poland*  
 (Received 26 May 1995)

In this paper we analyze theoretically the influence of the local-field effects on reflection spectra of a degenerate four-wave mixing in a dense medium of two-level atoms. We discuss the spectral dependence of the nonlinear absorption and dispersion of the signal and probe fields as well as their coupling for various strengths of the external field and atomic densities. For weak external fields the local-field effects reduce to the well known Lorentz redshift of the reflection spectra. When the external field saturates the transition in a dense sample significant modifications of the probe reflectivity and of the wave mixing spectra occur, resulting in asymmetric, multipeak line shapes. [S1050-2947(96)04807-X]

PACS number(s): 42.65.Hw, 42.62.Fi

### I. INTRODUCTION

Degenerate four-wave mixing (DFWM) has become a very useful tool for numerous applications, such as, e.g., phase conjugation, Doppler-free spectroscopy [1], and three-dimensional (3D) diagnostics of flames [2,3]. One of the fields where DFWM is particularly useful is plasma spectroscopy. Derivation of reliable spectroscopic information from plasmas is not an easy task because of the very complex nature of the plasma samples, which contain many neutral and charged particles excited to a large manifold of energy states, are strongly perturbed by collisions and electrostatic fields, and are spatially very inhomogeneous. On the other hand, determination of the local concentrations of a given species excited to a given internal state is essential for plasma diagnostics. This goal can be achieved with DFWM, which yields signals that are related to the populations of the *lower* states of the studied transitions, i.e., to the concentrations of the ground and metastable states, necessary for plasma diagnostics. DFWM is thus complementary to standard emission spectroscopy, which yields information on the *upper* states. Moreover, DFWM in the so-called backward geometry results in phase-conjugate signals. Such signals allow local, 3D mapping of a given species with a very good signal-to-noise ratio [4,5], which is very important in such inhomogeneous and turbulent media as plasma discharges.

Standard theoretical approaches to DFWM usually assume that the resonance medium is optically thin [1,6]. This may not be true in atmospheric pressure plasmas, where the density of metastable states can exceed  $10^{14} \text{ cm}^{-3}$ . One of the most important consequences of high density of optical media is the local-field effects that arise from the departure of the local fields from the external ones. Such a difference is theoretically described by the well-known Clausius-Mossotti or Lorentz-Lorenz relations [7] derived for quasistationary fields. This difference is also taken into account in the domain of nonlinear optical interactions by suitable correction factors [8] which were verified experimentally for nonresonant conditions and rather low densities [9]. On the other hand, several theoretical calculations [10] have recently been performed that predict very interesting behavior, such as an enhancement of refractive index [11], piezophotonic switch-

ing [12], mirrorless optical bistability [13], and others.

In this paper we wish to discuss the consequence of the local-field effects on DFWM spectra. The local-field effects in DFWM have already been analyzed in the forward geometry [14,15], however, as far as we are aware, no corresponding treatment has been given for the backward geometry. It is thus the purpose of this paper to analyze the phase-conjugate DFWM spectra under such conditions where the local-field effects are relevant.

Our analysis is performed within the standard classical approach with undepleted pump fields, two-level atoms, and with the slowly varying envelope approximation (SVEA). These rather strong assumptions considerably limit the applicability of our model. We think, nevertheless, that despite its simplicity the present study shows the most essential modifications of the DFWM spectra in the backward geometry due to the local-field effects. We neglect the effects of the Doppler broadening and pressure-induced resonances and concentrate mainly on the modifications which the local-field effects cause in the spectral responses of saturable, resonant media with respect to the case of optically thin samples, and which are very important for plasma diagnostics.

### II. CALCULATIONS

#### A. Atomic polarization

For calculation of the DFWM signal for a dense sample we take the local field as given by the Lorentz-Lorenz equation:

$$E_{\text{loc}} = E_{\text{ext}} + \frac{1}{3\epsilon_0} P, \quad (1)$$

where  $P$  is the macroscopic polarization of the sample and  $E_{\text{ext}}$  includes all external fields in the medium. Inserting  $E_{\text{loc}}$  into the Bloch equations one can calculate density matrix elements responsible for linear and nonlinear response.

We start from the Bloch equations with the driving local field:

$$\frac{\partial n}{\partial t} = -(n - n_0)\Gamma + i(\Omega_{\text{loc}}^* p - \Omega_{\text{loc}} p^*), \quad (2)$$

$$\frac{\partial p}{\partial t} = -(i\delta + \gamma)p + in\Omega_{\text{loc}}/2, \quad (3)$$

where  $n$  is the population difference;  $p$  is the atomic polarization given by equation  $P = N\mu p$ ,  $N$  being atomic density and  $\mu$  the dipole matrix element;  $\Omega_{\text{loc}}$  is the Rabi frequency of the total field acting on a given atom;  $\delta = \omega_L - \omega$  is the detuning of the laser frequency  $\omega_L$  from the atomic resonance at  $\omega$ ;  $\Gamma$  and  $\gamma$  are, respectively, the inverse longitudinal and transverse relaxation times; and  $n_0$  is the initial population difference caused by noncoherent pumping, such as, e.g., atom-atom and atom-electron collisions.

Equations (2) and (3) can be easily transformed to the form

$$\frac{\partial n}{\partial t} = -(n - n_0)\Gamma + i(\Omega^*p - \Omega p^*), \quad (4)$$

$$\frac{\partial p}{\partial t} = -[\gamma + i(\delta - \gamma Kn)] + in\Omega/2, \quad (5)$$

where  $\Omega$  is the spatially dependent Rabi frequency arising from the *external* field and  $K = N\mu^2/(6\varepsilon_0\hbar\gamma)$  is the coefficient characterizing the influence of the *local* fields in the medium.  $K$  is the dimensionless ratio of the Rabi frequency of the additional field, arising from the polarization of the other atoms in the medium, to the linewidth of the studied transition, i.e., it plays the role of a saturation parameter associated with the atomic field.

Steady-state solutions of such equations are

$$n = \frac{n_0(\Delta^2 + 1)}{\Delta^2 + 1 + S}, \quad (6)$$

$$p = \frac{\Omega}{2\gamma} \frac{(\Delta + i)n_0}{\Delta^2 + 1 + S}, \quad (7)$$

where  $\Delta = \delta/\gamma - Kn$ , and  $S$  is the spatially dependent saturation coefficient defined as  $S = |\Omega|^2/\Gamma\gamma$ .

These calculations are valid for the local response to any applied field in a dense medium of two-level atoms. In the case of four-wave mixing the spatial dependence of the applied fields must be considered. In this paper we consider the backward DFWM with two *counterpropagating* strong pump fields (with wave vectors  $\vec{k}_1$  and  $\vec{k}_2 = -\vec{k}_1$ ) and a weak probe (wave vector  $\vec{k}_3$ ) and signal (wave vector  $\vec{k}_4 = -\vec{k}_3$ ) fields propagating under a finite angle to the pump beams (Fig. 1) and assume no pump depletion. This assumption allows perturbative treatment of the probe and signal contributions to

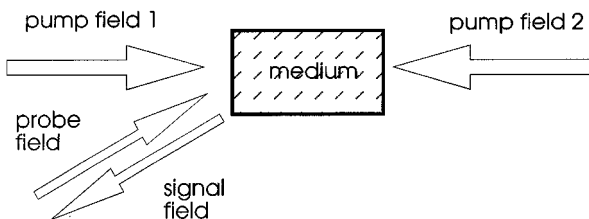


FIG. 1. Scheme of the backward DFWM experiment.

the whole polarization of the medium, i.e., taking the atomic polarization as linear in these weak-field amplitudes:

$$p \approx [p]_{E_{3,4}=0} + \left[ \frac{\partial p}{\partial \Omega} \right]_{E_{3,4}=0} \frac{\mu}{\hbar} (E_3 e^{i\vec{k}_3 \cdot \vec{r}} + E_4 e^{i\vec{k}_4 \cdot \vec{r}}) + \left[ \frac{\partial p}{\partial \Omega^*} \right]_{E_{3,4}=0} \frac{\mu}{\hbar} (E_3^* e^{-i\vec{k}_3 \cdot \vec{r}} + E_4^* e^{-i\vec{k}_4 \cdot \vec{r}}). \quad (8)$$

The coefficients in (8) are given as

$$\frac{\partial p}{\partial \Omega} = \frac{n_0}{2\gamma M^2} [\Delta(\Delta^2 + 1) + Kn_0SD(1 + S - \Delta^2)] + i \frac{n_0}{2\gamma M^2} [\Delta^2 + 1 - 2Kn_0SD\Delta], \quad (9)$$

$$\frac{\partial p}{\partial \Omega^*} = -\frac{n_0\Omega^2}{2\gamma^2 M^2 \Gamma} [\Delta + Kn_0D(\Delta^2 - 1 - S)] - i \frac{n_0\Omega^2}{2\gamma^2 M^2 \Gamma} [1 - 2Kn_0D\Delta], \quad (10)$$

where

$$M = \Delta^2 + 1 + S, \quad (11)$$

$$D = \frac{\Delta^2 + 1}{(\Delta^2 + 1 + S)^2 + 2Kn_0\Delta S}. \quad (12)$$

Since  $\Omega$  and  $S$  are spatially dependent in the standing pump field, atomic polarization  $p$  is also spatially dependent and has to be averaged over the standing-wave period when calculating the field amplitudes. While such averaging is quite straightforward in the standard case of a low-density sample, it cannot be performed analytically when local-field effects are important and has to be done numerically.

For very high densities and low saturation, an additional difficulty arises, that the absorption becomes significant already on a scale of  $\lambda$ . The standing-wave light pattern and the light-induced polarization and population gratings are hence seriously deformed for small  $\delta$ . It is important to realize that even in such high-density cases, the DFWM signals can be, at least qualitatively, calculated along the above lines. The direction of the reflected beam is still  $-\vec{k}_3$ , since the phase-matching condition responsible for the phase-conjugate response,  $\vec{k}_4 = \vec{k}_1 + \vec{k}_2 - \vec{k}_3$ , is fulfilled on the level of a single atom and, unlike its amplitude, does not depend on the grating quality. Also, when averaging individual atomic responses over the distorted standing wave, some intermediate value between zero and maximum field is obtained, qualitatively not very much different from the low-density case.

To get more insight into the local-field effects in DFWM it is instructive to compare Eqs. (9) and (10) with the corresponding coefficients for the case of  $K=0$ , i.e., without the local-field corrections:

$$\frac{\partial p}{\partial \Omega} = \frac{n_0\delta_n(\delta_n^2 + 1)}{2\gamma(\delta_n^2 + 1 + S)^2} + i \frac{n_0(\delta_n^2 + 1)}{2\gamma(\delta_n^2 + 1 + S)^2}, \quad (13)$$

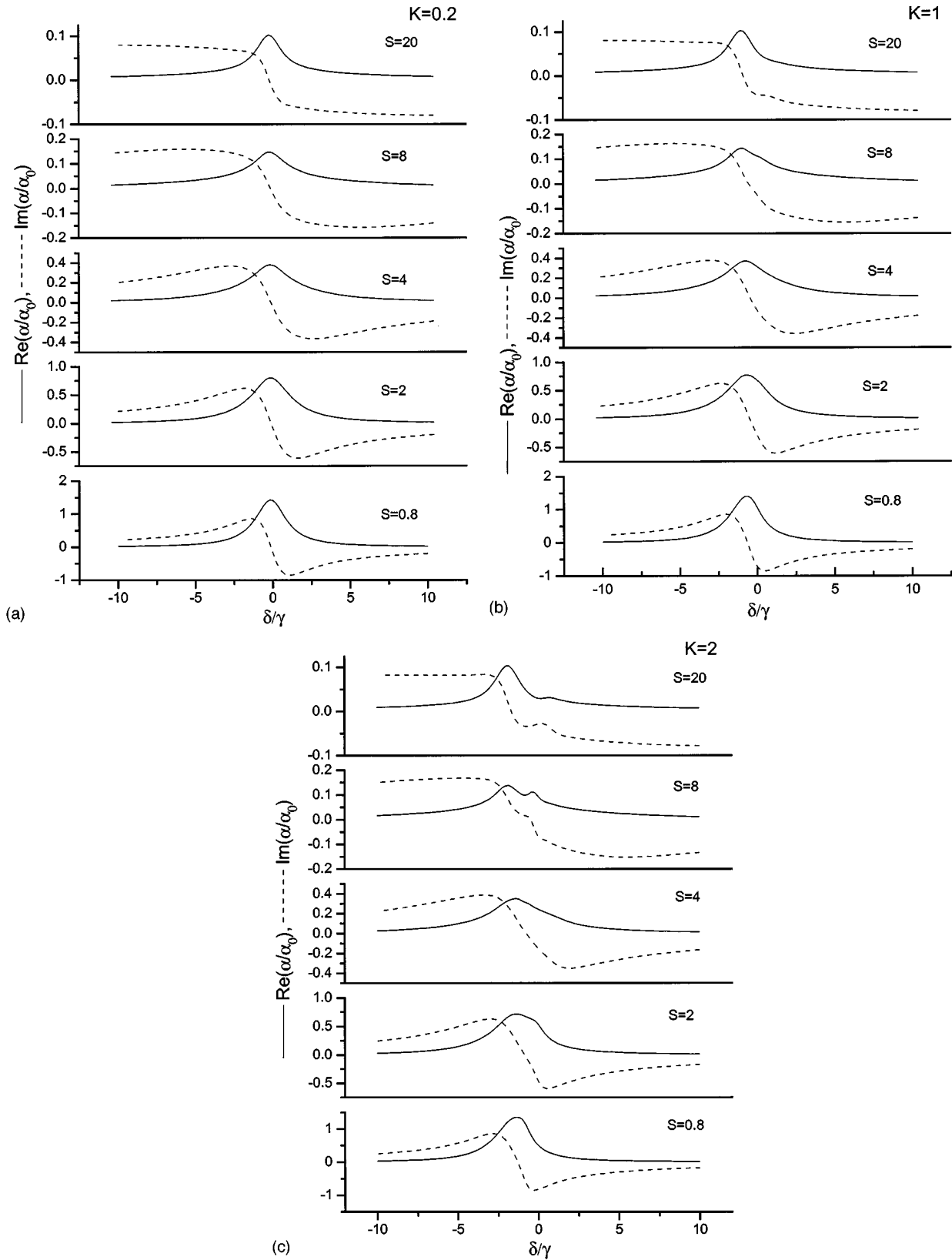


FIG. 2. Absorption ( $\text{Re}\alpha$ , solid line) and dispersion ( $\text{Im}\alpha$ , dashed line) coefficients calculated with local-field corrections for (a)  $K=0.2$ , (b)  $K=1$ , (c)  $K=2$ .

$$\frac{\partial p}{\partial \Omega^*} = -\frac{n_0 \delta_n \Omega^2}{2\gamma^2(\delta_n^2 + 1 + S)^2 \Gamma} - i \frac{n_0 \Omega^2}{2\gamma^2(\delta_n^2 + 1 + S)^2 \Gamma}, \quad (14)$$

where  $\delta_n = \delta/\gamma$  is the detuning normalized to the linewidth of the studied transition. From this comparison of Eqs. (9) and (10) with (13) and (14) one can easily see that the local-

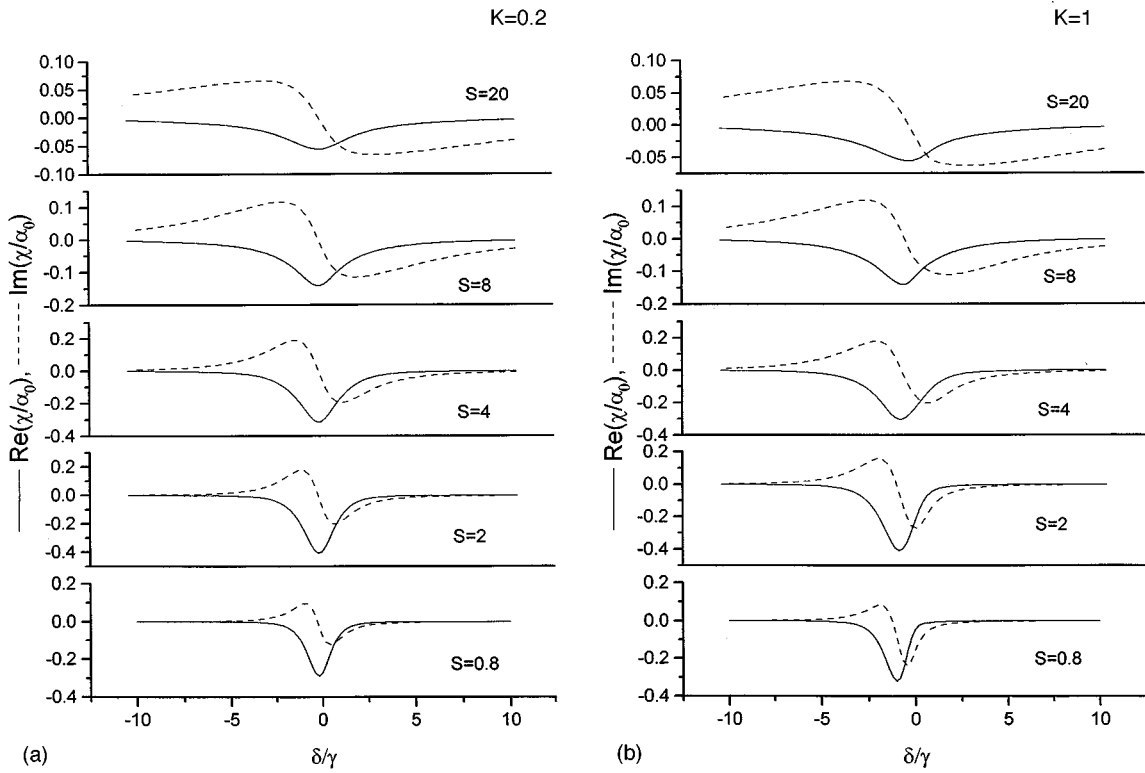


FIG. 3. Coupling coefficients calculated with local-field corrections for (a)  $K=0.2$ , (b)  $K=1$ , (c)  $K=2$ .

field corrections add asymmetric dispersive line-shape contributions to the symmetric absorptive curves and absorptive admixtures to the dispersive line shapes. As will be shown in the following section, such modifications can completely change the wavelength dependence of the wave-coupling coefficients and the line shapes of the reflection spectra.

### B. Wave propagation

We start with the wave equation in a dielectric, nonmagnetic medium in the form

$$\frac{\partial^2 E}{\partial z^2} = \mu_0 \epsilon_0 \frac{\partial^2 E}{\partial t^2} + \mu_0 \frac{\partial^2 P}{\partial z^2}. \quad (15)$$

Exact solution of the backward DFWM problem with local-field effects for an arbitrary thick medium is very difficult. In this work, we take a simplified approach with the SVEA and undepleted pump approximation (UPA). Though these are standard assumptions in most cases of nonlinear optics without local-field effects, their applicability for a thick medium is an open question. We make these assumptions bearing in mind that the results obtained would be reliable only for very short samples. Since the absorption depends on  $\delta$  and  $S$  like  $(1 + \delta_n^2 + S)^{-2}$ , the SVEA and UPA work satisfactorily also for frequencies far from resonance  $\delta_n \gg 1$  and strong saturation. The coupled-wave equations for the amplitudes of the probe and signal waves  $E_3$  and  $E_4$  are then obtained in the form

$$\frac{\partial E_3}{\partial z} = \alpha E_3 + \chi E_4^*, \quad (16)$$

$$-\frac{\partial E_4}{\partial z} = \alpha E_4 + \chi E_3^*, \quad (17)$$

where  $\alpha$  is the complex coefficient referring to absorption of a given wave, and  $\chi$  is the wave-coupling coefficient.

Extracting the parts of wave vectors  $\vec{k}_3, \vec{k}_4$  from the total atomic polarization  $p$  we can easily calculate coefficients  $\alpha$  and  $\chi$  :

$$\alpha = -i\alpha_0 \frac{\partial p}{\partial \Omega}, \quad (18)$$

$$\chi = -i\alpha_0 \frac{\partial p}{\partial \Omega^*}, \quad (19)$$

with  $\alpha_0 = N\mu^2\omega_L/(\epsilon_0\hbar\gamma c)$  being the linear absorption coefficient for the waves of frequency  $\omega_L$ .

Solving the coupled-wave equations (16) and (17) we can obtain intensity reflection coefficient  $R = |E_4/E_3|_{z=0}^2$  :

$$R = \frac{|\chi|^2}{|w \coth(wL) - \text{Re}\alpha|^2}, \quad (20)$$

with  $w = \sqrt{(\text{Re}\alpha)^2 - |\chi|^2}$ .

Equation (20) shows that  $R$  depends in a complex way on  $\alpha$  and  $\chi$ . Since, as discussed above, the local-field corrections seriously modify the symmetry of the spectral depen-

dences of the real and imaginary parts of  $\alpha$  and  $\chi$ , they also drastically affect the line shapes of the reflection spectra.

### III. RESULTS AND DISCUSSION

Our calculations of the DFWM spectra were performed by assuming very short interaction length,  $L \approx \lambda$ , to make the approximations more realistic. Such a limitation of  $L$  could be useful for 3D plasma diagnostics with high spatial resolution. Values of  $K$  were taken not bigger than 2 to avoid the risk of obtaining more than one solution for the population difference. The population difference is determined by a third-order algebraic equation, hence for sufficiently big  $K$  it can have three real roots for  $n$  which makes the  $n(S)$  dependence undetermined. This causes the so-called intrinsic optical, or mirrorless, bistability [13], which is beyond the scope of this work.

The values of the relevant physical parameters used in the present analysis are as follows:  $\mu = 10^{-29}$  C m,  $N = 10^{22} - 10^{23}$  m $^{-3}$ ,  $\gamma = \Gamma/2 = 2 \times 10^9$  s $^{-1}$ ,  $L = 10^{-6}$  m,  $\alpha_0 = 5 \times (10^6 - 10^7)$  m $^{-1}$ . By taking  $\gamma = \Gamma/2$  we assume pure radiative relaxation. However, allowing another relation between  $\gamma$  and  $\Gamma$ , such that  $\gamma > \Gamma/2$ , collisions can also be easily accounted for. While absolute values of the DFWM reflectivity depend on this relation, the effects of local fields on the DFWM signals have the same character in the case of collisional relaxation as in the case of  $\gamma = \Gamma/2$ , so we consider only the case of radiative relaxation here.

We start with the discussion of the spectral dependence of the nonlinear absorption and dispersion of the signal and probe fields, reflected in  $\alpha(\delta)$ , as well as their coupling, represented by  $\chi(\delta)$ .

For very small values of  $K$ , e.g.,  $K = 0.2$ , the line shapes of  $\alpha(\delta)$  and  $\chi(\delta)$  [Figs. 2(a) and 3(a)] do not differ much from the shapes calculated without local-field corrections. The real parts of both coefficients (solid lines) have absorptive character and the imaginary parts (broken lines) are dispersive-like. It is worth noting that the widths of  $\alpha(\delta)$  and  $\chi(\delta)$  have different saturation dependences in the range  $S = 0.8 - 20$ ; the width of  $\text{Re}\alpha$  does not change much with the saturation parameter, whereas the opposite is true for the width of  $\text{Re}\chi$ ; the width of  $\text{Im}\chi$  is comparable to the width of  $\text{Re}\chi$  but in  $\text{Im}\alpha$  two line-shape contributions could be recognized for high  $S$ , one of which becomes much broader than  $\text{Re}\alpha$ .

For  $K = 1$  [Figs. 2(b), 3(b)], the redshift of  $\alpha$  and  $\chi$  becomes noticeable. While the shift of  $\alpha$  is almost independent of saturation, the shift of  $\chi$  clearly decreases with increasing  $S$ . In addition to the features seen already at  $K = 0.2$ ,  $\text{Re}\chi$  ( $\text{Im}\chi$ ) loses its even (odd) symmetry.

For  $K = 2$  [Figs. 2(c), 3(c)], the redshift of  $\alpha$  and  $\chi$  becomes significant and the line shapes of the two coefficients undergo further deformations: for small saturation ( $S = 0.8$ ) they appear as nearly the same, 50:50 mixtures of the absorptive and dispersive contributions, and for strong saturation they acquire additional peaks. The appearance of these new structures cannot be related to any particular singularity of the spectral response of  $\alpha$  and/or  $\chi$ . This is due to different saturation dependences of the absorptive and dispersive line-shape coefficients given by Eqs. (13) and (14).

In Figs. 4(a) and 4(b), the calculated DFWM spectra, i.e.,

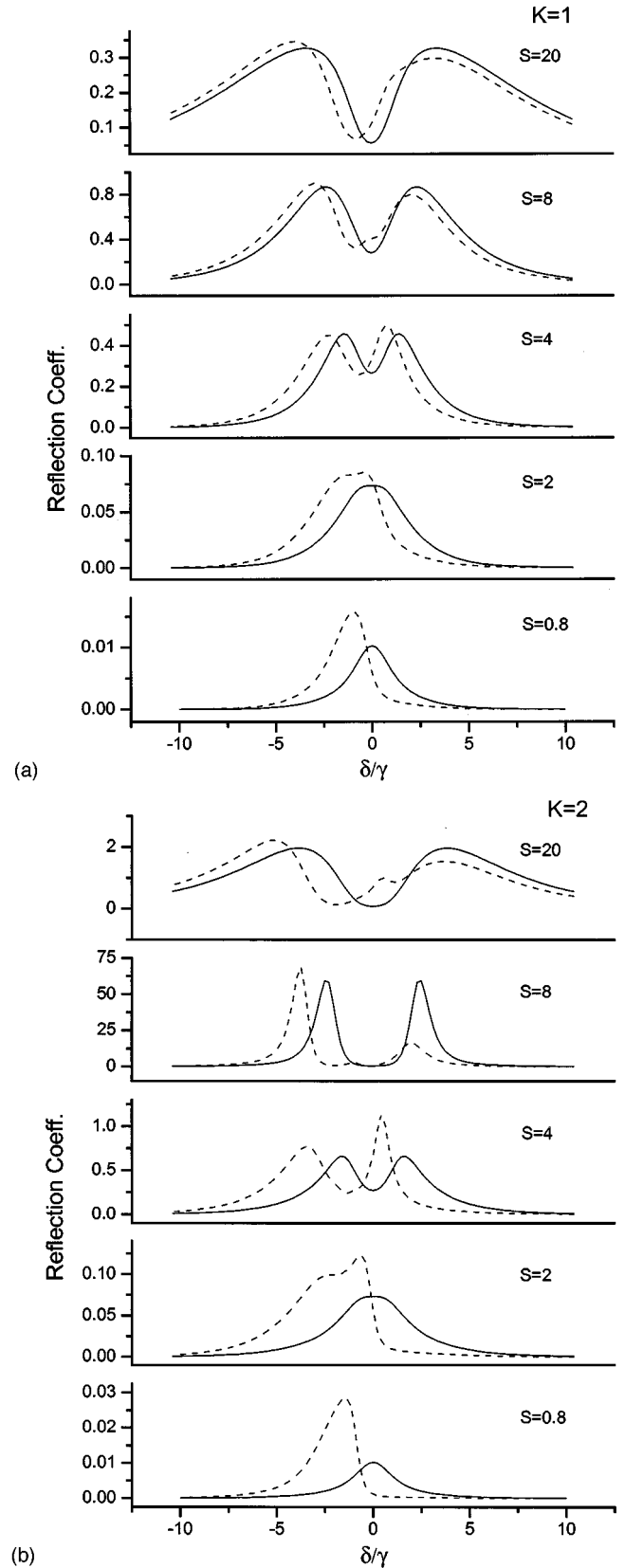


FIG. 4. Comparison of the reflection coefficients calculated with (dashed lines) and without (solid lines) local-field corrections for (a)  $K = 1$ , (b)  $K = 2$  and various values of  $S$ .

the  $R(\delta)$  plots, are displayed for various values of  $K$  and  $S$ .  $K$  is changed by changing the value of  $N$ , so even the spectra without local-field effects (dashed lines) differ for

different values of  $K$  because the corresponding values of  $\alpha_0$  also differ (spectra without local-field correction were calculated by setting  $K=0$ , but not  $N=0$ ).

For saturation below  $S=1$ , the effect of the local fields appears as the Lorentz redshift of the DFWM line, its slightly asymmetric shape, and a considerable increase of the reflection coefficient [Figs. 2(a) and 2(b)]. This increase can be easily understood as due to the enhancement of the net (local) field acting on atoms (not to be confused with the local-field enhancement factor [8,9]). For bigger external fields,  $S>2$ , in addition to the redshift, single lines split into two peaks that have equal amplitudes without local-field corrections but become clearly asymmetrical when local-field effects are relevant. Without local-field effects ( $K\ll 1$ ) the splitting has been explained physically by Woerdman and Schuurmans as the result of different saturation behavior of absorptive and dispersive parts of the light-induced polarization [16]. A similar explanation could be given for the case of  $K\approx 1$  when, as can be seen by comparison of Figs. 3 and 4, saturation changes the line shapes of  $\alpha(\delta)$  and  $\chi(\delta)$  in a different way. Also appearance of the third peak in the reflection spectra with  $K=2$  and  $S=20$  [Fig. 2(b)] can be associated with the new structures seen in the corresponding  $\alpha(\delta)$  and  $\chi(\delta)$  dependences. It is interesting to notice in Fig. 2 that, similarly to the case without local-field effects [16,17], the values of  $R$  calculated for given  $\delta$  increase with the light intensity for small  $S$  but drop down after reaching some maximum. Close to this maximum, strong narrowing of the  $R(\delta)$  spectra occurs which we attribute to the propagation effects.

#### IV. CONCLUSIONS

The backward resonant degenerate four-wave mixing is particularly important because of its applications to atomic and molecular spectroscopy and deserves detailed consideration. Most previous experimental works on the backward four-wave mixing were interpreted in terms of the Abrams and Lind theory [6] applicable to an optically thin medium of two-level atoms and not appropriate in the case of strong lines and dense media. Our calculations implement the local-field correction to the standard FWM equations and predict serious modifications of the spectral characteristics of the

backward four-wave mixing signals due to local-field effects in dense media. Since we also make SVEA and UPA, the present treatment should be regarded as a guide or a standard of comparison with more refined calculations and/or experimental data. Despite our, rather strong, assumptions, we believe that the results obtained reconstruct, at least qualitatively, the most significant modifications of the DFWM spectra due to the local-field effects. We show in this work that local-field corrections could easily modify the values of the reflection coefficients by more than 100% and that the redshift can significantly change the reflection spectra. While under usual experimental conditions parameter  $K$  seldom reaches the values of the order of 1 and the local-field corrections are not very big, large values of  $K$  could be reached under the following conditions.

(i) Typical transition with  $\mu=10^{-29}$  C m, and  $\gamma=2\times 10^9$  s $^{-1}$  in a very dense medium with the lower state density of about  $10^{23}$  m $^{-3}$ . These conditions can be fulfilled by some lines in a very hot, atmospheric pressure plasma.

(ii) Very strong transition with a small width, e.g., the helium 587.6 nm line ( $1s2p3P^0-1s3d^3D$  transition), with  $\mu=10^{-27}$  C m, and  $\gamma\approx 10^8$  s $^{-1}$ . For such a line  $K=1$  can be reached already for the lower state density of about  $10^{17}$  m $^{-3}$  which is feasible in a rf helium discharge [18].

It is worth noting that although most optical spectroscopic parameters, e.g., the optical thickness of the medium, derived without local-field corrections depend on the product  $NL$ , this is not true for the DFWM signals from the dense media, even in the low-signal regime. Such DFWM signals with the local-field contributions exhibit nonlinear dependence on  $N$  and are not proportional to  $NL$ . This is due to the fact that the local fields which affect the signals are themselves proportional to  $N$  and do not depend on  $L$ . The notion of optical thickness is hence meaningless when local-field effects are significant.

#### ACKNOWLEDGMENTS

This work was supported by the Polish Committee of Scientific Research (Grant No. 2 P302 052 05) and by the COST Scheme of the European Union (Grant No. CIPA-CT93-0094).

- 
- [1] *Optical Phase Conjugation*, edited by R. A. Fisher (Academic, New York, 1983).
- [2] T. Dreier and D. J. Rakestraw, *Opt. Lett.* **15**, 72 (1990).
- [3] T. Dreier and D. J. Rakestraw, *Appl. Phys. B* **50**, 479 (1990).
- [4] P. Ewart, P. Snowdon, and I. Magnusson, *Opt. Lett.* **14**, 563 (1989).
- [5] D. J. Rakestraw, R. L. Farrow, and T. Dreier, *Opt. Lett.* **15**, 709 (1990).
- [6] R. L. Abrams and R. C. Lind, *Opt. Lett.* **2**, 94 (1978); **3**, 205(E) (1978).
- [7] H. A. Lorentz, *The Theory of Electrons*, 2nd ed. (Dover, New York, 1952), Secs. 117–136 and Note 54.
- [8] N. Bloembergen, *Nonlinear Optics* (Benjamin, New York, 1965).
- [9] J. J. Maki, M. S. Malcuit, J. E. Sipe, and R. W. Boyd, *Phys. Rev. Lett.* **67**, 972 (1991).
- [10] C. M. Bowden and J. P. Dowling, *Phys. Rev. A* **47**, 1247 (1993).
- [11] M. O. Scully, *Phys. Rev. Lett.* **67**, 1855 (1991).
- [12] A. S. Manka, J. P. Dowling, C. M. Bowden, and M. Fleischhauer, *Phys. Rev. Lett.* **73**, 1789 (1994).
- [13] F. A. Hopf, C. M. Bowden, and W. H. Louisell, *Phys. Rev. A* **29**, 2591 (1984); B. A. Samson and W. Gawlik, *ibid.* **52**, R 4352 (1995).

- [14] R. Friedberg, S. R. Hartmann, and J. T. Manassah, *Phys. Rev. A* **40**, 2446 (1989).
- [15] R. Friedberg, S. R. Hartmann, and J. T. Manassah, *Phys. Rev. A* **42**, 494 (1990).
- [16] J. P. Woerdman and M. F. H. Schuurmans, *Opt. Lett.* **6**, 239 (1981).
- [17] R. L. Abrams, J. F. Lam, R. C. Lind, D. G. Steel, and P. F. Liao, in Ref. [1], pp. 211–284.
- [18] K. E. Greenberg and G. A. Hebner, *J. Appl. Phys.* **73**, 8126 (1993).